

# Effects of a Collective Spin Resonance Mode on the STM Spectra of D-Wave Superconductors

Jian-Xin Zhu,<sup>1</sup> Jun Sun,<sup>2</sup> Qimiao Si,<sup>2</sup> and A. V. Balatsky<sup>1</sup>

<sup>1</sup>Theoretical Division, MS B262, Los Alamos National Laboratory, Los Alamos, New Mexico 87545

<sup>2</sup>Department of Physics & Astronomy, Rice University, Houston, TX 77005

A high-energy spin resonance mode is known to exist in many high-temperature superconductors. Motivated by recent scanning tunneling microscopy (STM) experiments in superconducting  $B_{12}Sr_2CaCu_2O_{8+}$ , we study the effects of this resonance mode on the local density of states (LDOS). The coupling between the electrons in a d-wave superconductor and the resonance mode produces high-energy peaks in the LDOS, which displays a two-unit-cell periodic modulation around a non-magnetic impurity. This suggests a new means to not only detect the dynamical spin collective mode but also study its coupling to electronic excitations.

PACS numbers: 74.25.Jb, 74.50.+r, 74.20.-z, 73.20.Hb

A prominent feature in the excitation spectrum of the high- $T_c$  superconductors is the \41 meV" collective spin resonance mode, seen by inelastic neutron scattering experiments in most of the cuprate families [1, 2, 3, 4]. The physics of this resonance mode { including its microscopic origin, its connections with other physical properties, as well as its role on superconductivity itself { has been the subject of considerable debate. Given the recent developments of the atomic resolution scanning tunneling microscopy (STM) [5, 6, 7, 8, 9], it is timely to address the possible manifestation of this resonance mode in the local density of states (LDOS). A number of theoretical works [10, 11, 12, 13] have addressed the effect of related spin fluctuations on the LDOS. These works focused on the pinning of the spin fluctuations by impurity: a dynamical spin mode centered around the wavevector  $Q$  leads to a  $2Q$  spatial modulation in the low-energy LDOS. This result is smoothly connected to what happens in the case of a static spin-density-wave ordering [14, 15]. However, for the resonance mode { which is sharply peaked at  $Q = (0, 0)$  { such effects would not be manifested [since  $2Q = (2, 2)$  is equivalent to  $(0, 0)$ ]. There are also works about scattering of non-interacting electrons from non-magnetic impurities [16, 17].

In this paper, we show that the coupling of d-wave quasiparticles to the resonance mode does produce spatial modulations in the LDOS around an impurity. The feature is located at relatively high energies,  $(\epsilon_0 + \epsilon_0)$ , where  $\epsilon_0$  is the maximum superconducting energy gap and  $\epsilon_0$  the resonance energy. In addition, the wavevector of the LDOS modulation is close to  $Q = (0, 0)$ . Our predictions could be observable by the STM experiments. Such STM studies represent a new means to characterize the coupling between the electronic excitations and the resonance mode. The STM feature we discuss relates to the "peak-dip-hump" structure of the angle resolved photoemission spectroscopy (ARPES) [18, 19, 20, 21]; the inference about the electron-spin coupling from the ARPES and related spectroscopies is a topic of recent controversy [20, 21] and we

hope that the STM studies we propose will shed new light on this important issue.

We start with a model Hamiltonian describing two-dimensional electrons coupled to a collective spin mode and in the presence of a single-site impurity:  $H = H_{BCS} + H_{sp} + H_{imp}$ . Here the BCS-type Hamiltonian for a uniform d-wave superconductor is given by  $H_{BCS} = \sum_{\mathbf{k}, \sigma} (\epsilon_{\mathbf{k}}) c_{\mathbf{k}}^{\dagger} c_{\mathbf{k}} + \sum_{\mathbf{k}} (\epsilon_{\mathbf{k}} c_{\mathbf{k}\#}^{\dagger} c_{\mathbf{k}\#} + \epsilon_{\mathbf{k}} c_{\mathbf{k}} c_{\mathbf{k}\#})$ , where  $c_{\mathbf{k}}^{\dagger}$  ( $c_{\mathbf{k}}$ ) creates (annihilates) a conduction electron of spin  $\sigma$  and wavevector  $\mathbf{k}$ ,  $\epsilon_{\mathbf{k}}$  is the normal state energy dispersion for the conduction electrons, the chemical potential, and  $\epsilon_{\mathbf{k}} = \frac{\pi}{2} (\cos k_x \cos k_y)$  the d-wave superconducting energy gap. The coupling between the electrons and the resonance mode is modeled by an interaction term  $H_{sp} = g \sum_i S_i$ , where the quantities  $g$ ,  $S_i$ , and  $S_i$  are the coupling strength, the electron spin operator at site  $i$ , and the operator for the collective spin degrees of freedom, respectively. The dynamics of the collective mode will be specified below. The impurity scattering is given by  $H_{imp} = U_0 \sum_{\mathbf{k}} c_0^{\dagger} c_0$ , where without loss of generality we have taken a single-site impurity of strength  $U_0$  located at the origin,  $\mathbf{r}_i = 0$ . By introducing a two-component Nambu spinor operator,  $\psi_{\mathbf{k}} = (c_{\mathbf{k}}; c_{\mathbf{k}\#}^{\dagger})^T$ , the matrix Green's function for the d-wave BCS Hamiltonian  $H_{BCS}$  is determined by  $G_0^{-1}(\mathbf{k}; i!_n) = \sum_{\mathbf{k}} \frac{i!_n}{\epsilon_{\mathbf{k}} - \epsilon_{\mathbf{k}\#} + i!_n}$ ; where  $\epsilon_{\mathbf{k}} = \epsilon_{\mathbf{k}}$  and  $i!_n = (2n + 1)!$   $T$  is the fermionic Matsubara frequency. We have also assumed that the d-wave pair potential is real.

For a homogeneous system, where only the inelastic scattering of quasiparticles from the collective mode occurs, we calculate the self-energy to the second order in the coupling constant (see Fig. 1b):

$$\begin{aligned} \hat{\gamma}(\mathbf{k}; i!_n) = & \frac{g^2 T}{8} \sum_{\mathbf{q}} \frac{X(\mathbf{q}; i!_n)}{q^2} \gamma_{\mathbf{q}}(i!_n) \\ & 3G_{0;11} G_{0;12} - (k - \mathbf{q}; i!_n - i!_1) \\ & G_{0;21} 3G_{0;22} \end{aligned}$$

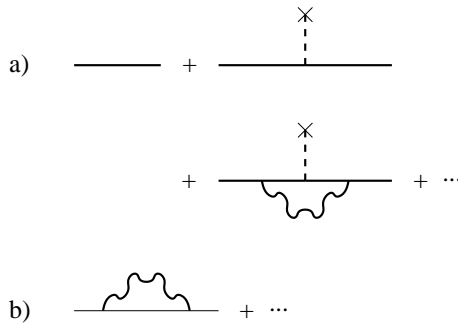


FIG. 1: a) Diagrams for  $G(p; p + q; !)$ . The thick solid line represents the full conduction electron Green's function in the absence of impurity,  $G_0$ . The dashed line is the coupling to an impurity, specified by a cross. The wavy line denotes the propagator of the collective mode; b) Self-energy diagrams for the conduction electrons in the absence of impurity,  $\hat{\Sigma}$ . The thin solid line is the bare (BCS) conduction electron Green's function,  $G_0$ .

where  $(q; i_1)$  is the dynamical spin susceptibility  $\epsilon_{ij}(q) = \hbar T \langle S_i^x(q) S_j^x(0) \rangle i$  and  $i_1 = 2\pi T$  the bosonic Matsubara frequency. The dressed Green's function is:

$$G_0^{-1}(k; i_1) = \begin{matrix} i_1 & n & k & 11 & k & 12 & \dots \\ & k & 21 & i_1 + k & 22 & & \end{matrix} : \quad (1)$$

The corresponding real-space dressed Green's function  $G_0(i; j; i_1)$  is obtained through a Fourier transform with respect to  $r_i - r_j$ . For the d-wave pairing symmetry, one can show that the local Green's function,  $\hat{G}_0(i; i_1)$  =  $G_0(i; i; i_1)$  is diagonal. In the presence of a single-site impurity at  $r_i = 0$  with potential strength  $U_0$ , the site-dependent Green's function can be written in terms of the T-matrix:

$$G(i; j; E) = \frac{G_0(i; j; E)}{X} + \frac{G_0(i; i; E) \hat{T}_{lm}(E) G_0(m; j; E)}{lm} : \quad (2)$$

Due to the vertex corrections induced by the coupling to the collective modes (Fig. 1a), the T-matrix in general contains site-off-diagonal terms. We will first carry out the calculation without the vertex corrections, in which case  $\hat{T}_{lm} = \hat{T}_{10, m; 0}$ , with  $\hat{T}^{-1} = U_0^{-1} \hat{G}_0$ , where  $\hat{G}_0$  is the z-component of the Pauli matrix. The LDOS at the  $i$ -th site is

$$\langle n_i(E) \rangle = -\frac{2}{\pi} \text{Im} G_{11}(i; i; E + i) ; \quad (3)$$

where  $i = 0^+$ .

Up to now, our discussion and formulation are quite general and can be applied to study the effects of any dynamical mode once the susceptibility is known. We treat the susceptibility in a phenomenological form (based on the inelastic neutron scattering observations), see

also [22]:

$$(q; i_1) = \frac{q\omega}{2} \frac{1}{i_1 - \omega_0} \frac{1}{i_1 + \omega_0} ; \quad (4)$$

where we denote the wavevector  $Q = (q, \omega)$  and the mode energy by  $\omega_0$ . This form is especially suitable for the optimally doped  $YBa_2Cu_3O_{6+y}$  (YBCO) compounds in the superconducting phase, where the observed neutron resonance peak is almost resolution-limited in energy and fairly sharp in wavevector. The resonance peak in BSCCO is broadened in both energy and wavevector. The finite width in the wavevector space might be important for the ARPES lineshape in general and in particular the understanding of the ARPES spectra away from the M points  $k = (0, 0)$  and symmetry-related points of the Brillouin zone [22], but should not change the qualitative conclusion of our work: the LDOS effects we will discuss arise from the fact that the dominant effects of the resonance mode on the single-electron spectral functions occur near the M points which is expected to remain to be the case beyond our simplified form for the susceptibility. In addition, given that the peak in BSCCO is still quite sharp in energy, we expect that the main effect of the broadening in energy of the resonance mode is to extend the bias window for the LDOS feature we will discuss. We have also neglected the incommensurate peaks seen in the inelastic neutron scattering experiments in YBCO (the part that disperses "downward" away from the resonance peak) [23, 24, 25, 26], since their spectral weight is significantly smaller than that of the resonance mode. For the normal-state energy dispersion, we use  $\epsilon_k = 2t(\cos k_x + \cos k_y) - 4t^0 \cos k_x \cos k_y$ , where  $t$  and  $t^0$  are the nearest and next-nearest neighbor hopping integral. Unless specified explicitly, the energy is measured in units of  $t$ . We choose  $t^0 = 0.2t$  to model the band structure of the hole-doped cuprates. Since the maximum energy gap for most of the cuprate superconductors at the optimally doping is about 30 meV while the resonance mode energy is in the range between 35 and 47 meV, we take  $\omega_0 = 0.1t$  and  $\omega_0 = 0.15t$  (i.e.,  $1.5\omega_0$ ). The chemical potential is tuned to give an optimal doping value 0.16. To mimic the intrinsic life-time broadening, in our numerical calculation we take  $\tau$  of Eq. (3) to be 0.04  $\omega_0$ . A system size of  $N_x = N_y = 1000$  is taken in the numerical calculation.

In the absence of impurities, the density of states is the summation of the spectral function,  $A_k(E) = \frac{2}{\pi} \text{Im} G_{0,11}(k; E + i)$ , over all wavevectors  $k$ . Fig. 2 (a) shows the spectral function at an M point of the Brillouin zone. Without the electron-mode coupling, as is well known, the spectral function is peaked at the maximum gap edges  $\omega_0$ . As the electron-mode coupling is switched on, new peaks emerge at the energies  $E_1 = (\omega_0 + \omega_0)$ . (For simplicity, we have neglected the broad "background" part of the single-electron spectral function in our consideration.) The peaks in  $A_k$  orig-

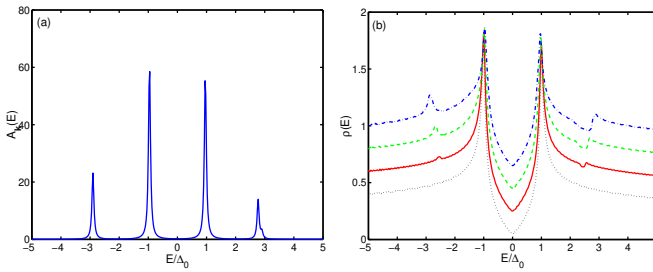


FIG .2: Spectral function  $A_k(E)$  at the wavevector  $k = (0, 0)$  for  $g=0 = 3$  (a). The density of states,  $p_k(E)$ , is shown in (b), for various values of  $g=0 = 0$  (black dotted line), 1 (red solid line), 2 (green dashed line), and 3 (blue dash-dotted line); here, for easier viewing, the consecutive curves are shifted by 0.2 along the vertical axis.

inate from the poles of the Green's function  $G_{0,11}$ . Note that the weight of the peak at  $E_0$  is larger than at  $E_1$  because the van Hove singularity is below the Fermi energy. Since the spectral weight of the spin resonance mode [i.e.,  $\text{Im}[\langle q; ! \rangle]$ ] is peaked at  $Q$ , the feature of the quasiparticle self-energy is the strongest around the  $M$  points of the zone because they are connected by  $Q$ . The singularity in the quasiparticle self-energy causes additional poles in the Green's function. As the coupling constant  $g$  increases, these peaks are shifted to higher energies and, in addition, their spectral weight is enhanced; simultaneously, the weight of the superconducting coherent peaks is reduced to obey the sum rule. The shift of states due to inelastic scattering is expected in DOS and is also expected for scattering of local mode [27]. Fig. 2(b) plots the density of states and clearly shows that the high energy peaks still occur around  $E_1$ . In other words, the contributions from near the  $M$  points dominate the wavevector summation for the density of states, reflecting the nature of the normal state band near this point. Furthermore, the highly asymmetric structure in the DOS at energies  $E_1$  and  $E_1$  comes from the singular structure in the quasiparticle self-energy. These results, for the clean case, are consistent with earlier studies [20, 21, 22].

We are now in a position to address the LDOS in the presence of a single nonmagnetic impurity. For concreteness, we take the on-site potential  $U_0 = 100$ . Fig. 3 shows the LDOS directly at the impurity site, as well as at its nearest neighbor. The near-zero energy resonant state triggered by the quasiparticle scattering from the impurity [28] is robust against the electron-mode coupling. Our key new results are two-fold. First, the impurity mode changes the shape of the spectral features at  $E_1$ , which can now be either a dip or a peak. Second, and more importantly, these high energy features at  $E_1$  exhibit a spatial dependence. At the impurity site, the LDOS displays a dip at  $E_1$  but a peak at  $+E_1$ . The behavior is reversed at the site closest to the impurity.

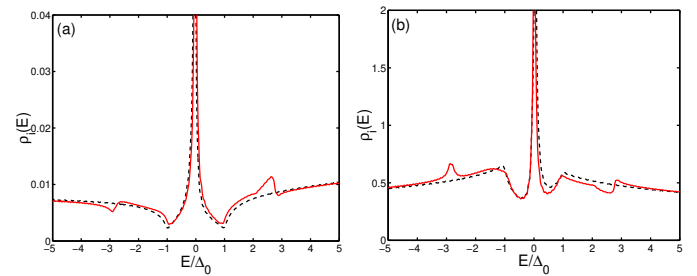


FIG .3: Local density of states at the impurity site (a) and at its nearest neighbor (b). The coupling constant  $g=0 = 3$ .

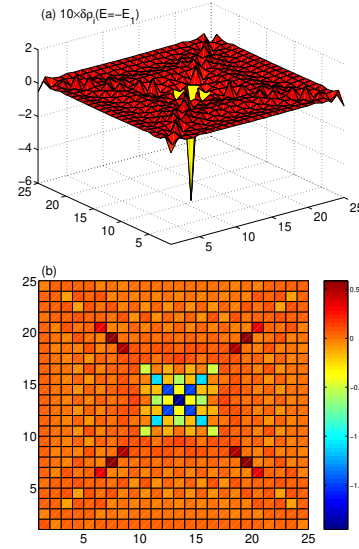


FIG .4: The spatial variation of the LDOS around the impurity with the mode coupling  $g=0 = 3$  (a), and the difference (b) between this LDOS and its counterpart with  $g = 0$ . The density of states is measured with respect to its spatial average value. The image window of  $25 \times 25$  plaquettes is taken from a system of size  $1000 \times 1000$ .

To explore this spatial variation of the LDOS in more detail, we have calculated the LDOS, with the energy fixed at  $E_1$ , in the vicinity of the impurity with and without the mode coupling. In the absence of mode coupling, we obtain the results (not shown) which are consistent with previous studies [28]: the LDOS exhibits a Friedel oscillation along the diagonals of  $\text{CuO}_2$  plane but no other non-trivial features. When the mode coupling is turned on, in addition to the Friedel oscillation along the diagonals, the LDOS displays a new type of modulation with a period of  $2a$  in the wide regions along the bond direction [Fig. 4(a)]. This new modulation can be seen more clearly by looking at the difference [Fig. 4(b)] between the LDOS shown in Fig. 4(a) and its counterpart in the absence of a mode coupling.

Alternatively, the new modulation can also be seen by performing a Fourier transform. However, the predom-

inant features in the field of view of Fig. 4 are not the new modulation, but the impurity-induced Friedel oscillations along the diagonals. In order to highlight the new modulation, we find it useful to perform a filtered Fourier transform,  $\langle \mathbf{q}; E \rangle = \sum_{\mathbf{i}}^0 e^{i\mathbf{q} \cdot \mathbf{i}} \langle \mathbf{i}; E \rangle$ , where  $\sum^0$  denotes a summation over all the sites shown in Fig. 4 (a) except for those located within two strips along the diagonals. [In other words, the Fourier transform is done using four disconnected triangles in the field of view.] This process filters out the signals associated with the Friedel oscillation, which is induced primarily by the impurity alone. The resulting Fourier-transformed image [29] is given in Fig. 5, which unambiguously shows that the new feature induced by the coupling to the spin resonance mode has a spatial modulation wavevector  $(\frac{1}{2}, \frac{1}{2})$ .

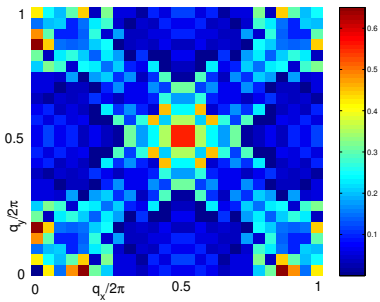


FIG. 5: The wavevector dependence of  $\langle \mathbf{q}; E_1 \rangle$ , the Fourier transform of Fig. 4 (a) after filtering out the LDOs at the sites inside two strips along the diagonals; see main text for details.

This new type of LDO modulation with a wavevector close to  $\mathbf{Q} = (\frac{1}{2}, \frac{1}{2})$  reflects the dominance of the collective mode effect near the M points of the Brillouin zone. It follows from Eqs. (2,3), with the form of the T-matrix under consideration and when the chosen field of view has an inversion symmetry with respect to the impurity site, that the Fourier-transformed LDOs for any finite  $\mathbf{q}$  is,

$$\langle \mathbf{q}; E \rangle = -\frac{1}{2} \text{Im} \int \text{d}\mathbf{p} \underline{\mathbf{G}}_0(\mathbf{p} + \mathbf{q}; E) \hat{\mathbf{T}}(E) \underline{\mathbf{G}}_0(\mathbf{p}; E) \quad (5)$$

At positive energies, the poles shown in Fig. 2 for  $\underline{\mathbf{G}}_0(\mathbf{p}; E)$  are located [18, 19, 20, 21, 22] at  $E_p$  and  $E_{p+q} + \omega_0$ , respectively. (Here,  $E_p = \sqrt{\frac{p_x^2}{2} + \frac{p_y^2}{2}}$ .) Likewise,  $\underline{\mathbf{G}}_0(\mathbf{p} + \mathbf{q}; E)$  is the sum of two poles, one at  $E_{p+q}$  and the other at  $E_{p+q} + \omega_0$ . At  $E = E_1$ , Eq. (5) is dominated by the convolution between the poles at  $E_{p+q} + \omega_0$  and  $E_{p+q} + \omega_0$ . This term in turn is dominated by the contributions corresponding to when both  $\mathbf{p} - \mathbf{Q}$  and  $\mathbf{p} + \mathbf{q} - \mathbf{Q}$  are near to the M points, leading to a  $\langle \mathbf{q}; E_1 \rangle$  that is peaked near  $(\frac{1}{2}, \frac{1}{2})$ .

We now briefly discuss the effect of the vertex corrections. The T-matrix would then need to be determined by solving an integralequation in the wavevector space. The vertex correction to the T-matrix to the same order ( $g^2$ ) of our calculation for the selfenergy is shown

in Fig. 1(a). It turns out to involve a wavevector convolution of a form similar to that given in Eq. (5). We therefore expect [30] an additive contribution to  $\langle \mathbf{q}; E_1 \rangle$  that is also peaked near  $(\frac{1}{2}, \frac{1}{2})$ .

To summarize, we have studied the effects of the magnetic resonance mode on the tunneling spectrum in the presence of a nonmagnetic impurity. The LDOs around the impurity displays resonant features at relatively high energies [close to  $(\frac{1}{2}, \frac{1}{2})$ ], which modulates in space with a wavevector close to  $(\frac{1}{2}, \frac{1}{2})$ . Our prediction can be tested straightforwardly by operating the existing high resolution STM at a relatively high energy window. Such studies should shed considerable new light on the physics of the spin resonance mode, in particular its coupling to the electronic excitations.

We are especially grateful to J. C. Davis for helpful conversations at the early stage of this work. The authors have benefited considerably from discussions with Ar. Abanov, Y. Bang, A. V. Chubukov, K. Damle, and M. Norman. This work was supported by the Department of Energy through the Los Alamos National Laboratory (JXZ and AVB), by TCSAM and the NSF Grant No. DMR-0090071 (JS and QS). JXZ also acknowledges the hospitality of the Rice University, where part of this research was carried out.

---

- [1] J. Rossat-Mignod et al, *Physica C* 185–189, 86 (1991).
- [2] H. A. Mook et al, *Phys. Rev. Lett.* 70, 3490 (1993); P. Dai et al, *Phys. Rev. B* 63, 054525 (2001).
- [3] H. F. Fong et al, *Phys. Rev. B* 54, 6708 (1996); *Nature* 398, 588 (1999).
- [4] H. F. He et al, *Phys. Rev. Lett.* 86, 1610 (2001); *Science* 295, 1045 (2002).
- [5] J. E. Hoffman et al, *Science* 266, 455 (2002).
- [6] J. E. Hoffman et al, *Science* 297, 1148 (2002).
- [7] C. Howard et al, cond-mat/0201546.
- [8] C. Howard et al, cond-mat/0208442.
- [9] K. M. McElroy et al, submitted to *Nature*.
- [10] A. Polkovnikov, M. Vojta, and S. Sachdev, *Phys. Rev. B* 65, 220509 (2002); cond-mat/0208334.
- [11] D. Podolsky et al, cond-mat/0204011.
- [12] J. H. Han, cond-mat/0206284.
- [13] S. A. Kivelson et al, cond-mat/0210683.
- [14] O. Zachar, S. A. Kivelson, and V. J. Emery, *Phys. Rev. B* 57, 1422 (1998).
- [15] J.-X. Zhu, I. Martin, and A. R. Bishop, *Phys. Rev. Lett.* 89, 067003 (2002); Y. Chen, H.-Y. Chen, and C. S. Ting, *Phys. Rev. B* 66, 104501 (2002).
- [16] Q.-H. Wang and D.-H. Lee, *Phys. Rev. B* 67, 020511(R) (2003).
- [17] D. Zhang and C. S. Ting, cond-mat/0209318.
- [18] D. S. Dossau et al, *Phys. Rev. Lett.* 66, 2160 (1991); Z. X. Shen and J. R. Schrieffer, *ibid.* 78, 1771 (1997).
- [19] J. C. Camuzano et al, *ibid.* 83, 3709 (1999); M. R. Norman and H. Ding, *Phys. Rev. B* 57, 11089 (1998).
- [20] Ar. Abanov et al, *Phys. Rev. Lett.* 89, 177002 (2002), and references therein.

[21] H.-Y. Kee, S. A. Kivelson, and G. Aeppli, Phys. Rev. Lett. 88, 257002 (2002).

[22] M. Eschrig and M. R. Norman, Phys. Rev. Lett. 85, 3261 (2000); M. Norman, private communication.

[23] M. Arai et al., Phys. Rev. Lett. 83, 608 (1999).

[24] H. F. Fong et al., Phys. Rev. B 61, 14773 (2000).

[25] J. Brinckmann and P. A. Lee, Phys. Rev. Lett. 82, 2915 (1999).

[26] Y.-J. Kao, Q. Si, and K. Levin, Phys. Rev. B 61, R11898 (2000).

[27] A.V. Balatsky, A.R. Abanov, and J.X. Zhu, cond-mat/0211448, and references therein.

[28] A.V. Balatsky, M.I. Salkola, and A. Rosengren, Phys. Rev. B 51, 15547 (1995); M.I. Salkola, A.V. Balatsky, and D.J. Scalapino, Phys. Rev. Lett. 77, 1841 (1996).

[29] Similar procedure for the LDOs in the absence of a mode coupling yields a Fourier-transformed LDOs that is featureless near  $(\vec{Q}; \omega)$ .

[30] We have numerically calculated the leading order vertex correction contribution to the LDOs, finding that it is indeed peaked near  $\vec{Q}$ .